"CHARACTERISTICS OF MOULD FLUX FILMS FOR CASTING MC AND LC STEELS"

Zushi Li[(1)]
Ken Mills [(2)]
Maria Carolina Campello Bezerra[(3)]

ABSTRACT
The characteristics of mould flux films developed while casting MC and LC steels taken from a continuous casting mould have been investigated. These characteristics include appearance, porosity, crystallinity, mineralogical phases, cross-sectional microstructure, and element distribution and thickness of solid/liquid layers. The following are discussed: (i) the effect of chemical compositions of mould fluxes on the characteristics of the films and (ii) the mechanisms responsible for crystallisation and porosity formation.
Two mould flux films for casting MC and LC steel grades were taken at around 300 mm from the top of the mould in the end of casting. The crystallinity of flux films was investigated by direct observation of optical microscope and SEM. XRD was used to detect the mineralogical phases in the mould flux films. The microstructure and cross-sectional element distribution were studied by SEM/SEM-EDS. The porosity and appearance of flux films were determined by imagine analysis system.
It was verified that the horizontal heat transfer between shell and mould is controlled by (i) thickness of the solid slag film and (ii) the surface roughness (equivalent to an air gap) formed when the initial glassy slag film crystallises. Both the surface roughness and the crystalline fraction (90%) of the slag film for casting MC grades were greater than those for casting LC grades. The crystalline fraction can be related to the flux composition by using the parameter "modified NBO/T". The mechanism for the crystallisation and porosity formation of the flux films is discussed.

Key words: Mould flux, Slag Films.

XXXV Seminário de Fusão, Refino e Solidificação dos Metais – 2004, May 17 to 19 2004 – Salvador, BA-Brazil

(1) Scientist of Department of Materials from Imperial College of Science, Technology and Medicine - London
(2) Professor and Scientist of Department of Materials from Imperial College of Science, Technology and Medicine - London
(3) Ceramic Technical, Production Engineer and Steel Making Product Manager of Carboox Resende Química.

1. INTRODUCTION

In continuous casting of steel, mould fluxes are added on the top of the mould to prevent thermal loss and reoxidation of liquid steel and to absorb floated liquid/solid inclusions from the liquid strand. The two most important roles of mould fluxes, *i.e.* lubrication of steel shell and heat transfer between steel shell and water-cooled copper mould are accomplished by mould flux films. Mould flux films are formed by the infiltration of molten mould flux into the gap between the water-cooled copper mould and the steel shell.

Mould flux for casting a certain steel grade is designed to meet the solidification requirements of that steel which is finally reflected in the characteristics of mould flux film. For example, mould flux for casting medium carbon steel is designed to have the slag film with high crystallinity (crystalline fraction) to create uniform heat transfer across the slag film and subsequently to reduce the longitudinal cracks in the cast product. In the case of casting low carbon steel at fast speed, the thin mould flux film with low crystallinity is required to get thick steel shell to prevent from sticker breakouts. Therefore, some investigations have been carried out on the mould flux films taken from continuous casters due to the importance of mould flux film in the efficient casting operation and subsequently the quality of cast products (Grieveson, Bagha et al. 1988; Susa, Mills et al. 1994; Courtney, Nuortie-Perkkio et al. 2001; Bezerra, Afrange et al. 2002; Hooli 2002; Tarrant and Brooks 2003).

Grieveson *et al.*(Grieveson, Bagha et al. 1988) determined the mineralogical constitution of the slag film from both simulation experiments and industrial continuous by X-ray analysis. Cuspidine ($3CaO\ 2SiO_2\ CaF_2$) is always present in the mould flux films except fluorine-very low or free mould fluxes. Other minor phases depending on the contents of Na_2O and Al_2O_3, may be wollastonite ($CaO\ SiO_2$), gehlenite ($2CaO\ Al_2O_3\ SiO_2$), nepheline ($Na_2O\ Al_2O_3\ 2SiO_2$), disodium alumino disilicate ($2Na_2O\ Al_2O_3\ 2SiO_2$), and combeite ($Na_4(Ca, Al, Fe)_3Si_6O_{16}(OH, F)_2$). Bezerra *et al.*(Bezerra, Afrange et al. 2002) found that cuspidine is always present in all the mould flux films, but fluorite and nepheline also appear in some mould flux films.

Several methods have been developed to correctly determine the crystallinity in the slag films(Courtney, Nuortie-Perkkio et al. 2001). These methods can be divided into direct observation using optical microscopy and electric microscopy, and comparative method such as DPSC (Differential Power Scanning Colorimeter), DTA, XRD. It is recommended that the crystallinity of the slag films should be determined by two or more methods, and the uncertainties in the measurements of the crystallinity are of the order of ±10%.

In order to analyse the mechanism of heat transfer between the steel shell and the mould, thermal properties of mould flux films were measured including thermal diffusivity, conductivity, heat capacity, absorption coefficient, refractive index and density(Susa, Mills et al. 1994).

Hooli(Hooli 2002) studied the structure and composition distribution in the mould flux films which were taken from the meniscus to 390 mm below the meniscus of the mould for casting stainless steel slabs. The flux films structure concerning different slag phases changes from the meniscus downwards. There are no significant changes in compositions of different layers from mould side to shell side near meniscus. However, farther away from the meniscus, large differences in composition developed. For example, the concentrations of sodium and fluorine can

be 50% in the film layer against mould for the sample taken from 390 mm below the meniscus of the mould.

Bezerra *et al.*(Bezerra, Afrange et al. 2002) analysed several slag film samples for different steel mills to evaluate the effect of the casting parameters (eg. Steel grade and mould flux composition) on the physical and chemical characteristics of these slag films.

Tarrant and Brooks (Tarrant and Brooks 2003) has investigated the mould flux films for casting MC, LC and SULC steel grades. The %crystallinity in these films were determined using XRD and micrograph image analysis, the mineral phases were detected to be cuspidine for all fluxes and nepheline for MC steel. Different crystal morphologies across the film thickness were also found.

In this study, characteristics of mould flux films for casting MC and LC steel grades taken from continuous casters were investigated using different techniques such as optical microscopy, SEM-EDS, XRD and image analysis. These characteristics include the appearance, porosity (bubble), crystallinity, element distribution between different mineral layers and thickness of the solid/liquid layers. The effects of steel grades and chemical compositions of the mould fluxes on the characteristics of mould flux films were discussed.

2. EXPERIMENTAL

Two mould flux films for casting MC and LC steel grades, denoted as A and B respectively, were taken at the end of casting. At the moment the steel level was lowered in the mould, the solidified slag film automatically peeled out from the mould wall. The samples were taken at around 300 mm from the top of the mould. The total height of the mould is 900 mm. The chemical composition and physical properties of the two mould fluxes and the operation conditions of continuous casting were shown in *Table 1*.

Table 1- Chemical compositions (%) and physical properties of mould fluxes A and B and operation conditions of continuous casting before the mould flux films were taken.

	Al_2O_3	R_2O	F	C/S	T_{br}, (C)	η_{1300} (poise)	Steel Grade	Mould dimension (mm)	Casting speed (m/min)	Consumption rate (kg/t)
A	7.47	6.21	8.13	1.28	1220	1.5	MC	1220×252	0.75	0.70
B	2.53	12.92	9.43	0.93	1050	1.1	LC	1435×252	1.00	0.58

The representative samples were mounted with expose resin, ground on SiC paper, and finally fine-polished with 1ìm diamond paste. The samples were etched with 2.5 vol% HF in distilled water for 2 s. The etched samples were observed in an optical transmission microscope under normal and polarised mode to reveal the glassy and crystalline areas.

Then the polished samples were coated with carbon. The carbon-coated samples were analysed using scanning electron microscope (SEM). The SEM is a JEOL 840, equipped with microanalysis system by energy dispersion link INCA 300 with SiLi detector, Oxford, Pentafet. All analyses were made using 20KV of electrons acceleration tension. The microanalysis resolution by EDS is about 1 to 2 μm of

surface range and about 1.5 to 5 μm of depth depending on materials density on the analyzed point.

The X-ray diffraction to determine the crystalline phases in mould flux films were performed using Philips PW 1710 X-ray generator with copper radiation, goniometer speeds of 0.04 /s. The diffraction spectrums were compared with ICDD-1996 standard.

The %crystallinity of the mould flux films was determined using differential power scanning calorimetry (DPSC) and direct observation using optical microscope and scanning electron microscope.

The porosity (bubble) was determined from the SEM photos using Neophot 21 equipped with Zeiss KS400 image analysis software (Carl Zeiss Vision GmbH). The pore diameter was calculated from the pore area assuming that the pore is a spherical hole. Only the pores with a diameter of larger than 5 μm were detected in this study. The porosity is also expressed as pore number per mm mould flux film in vertical direction in both mould side and shell side.

The same characteristic was obtained by observing more than three representative samples.

3. RESULTS

3.1 Sample appearance

The appearance of both samples A and B is shown in **Figure 1**. The whole cross section of mould flux film A is opaque, while mould flux film B is composed of an opaque layer against mould (30-40% in thickness) and a transparent greenish glassy layer against steel shell.

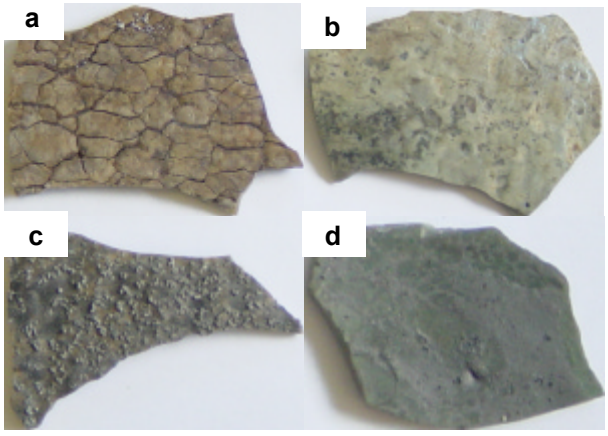

Fig.1 The appearance of mould flux films A and B.
a, b: the surface against mould of samples A and B;
c, d: the surface against shell of samples A and B.

Mould flux film A has a thickness ranging from 1.31mm to 3.51 mm with an average thickness of 2.41mm and a standard deviation of 0.47. The thickness of mould flux film B ranges from 1.24 mm to 1.90 mm with the average value of 1.63 mm and a standard deviation of 0.14. Thus the mould flux film for casting MC steel (sample A) is approximately 1.5 times thicker and with a wider distribution in

thickness than that for casting LC steel (sample B). The wide distribution in thickness of mould flux film A is mainly caused by the wave in the surface against mould and the side against steel shell is much flat.

As shown in **Figure 1(a)**, there are many network cracks in the surface against mould of sample A, with the width of less than 0.9 mm and the depth of less than 1.0 mm. The amount of network cracks is measured and expressed as the length of cracks in the unit surface area, that is, 0.47 mm/mm^2. But there are no network cracks in the surface against mould of sample B for casting LC steel.

3.2 Structure and porosity

Figure 2 shows the SEM cross-sectional microstructure of samples A and B. Both samples A and B can be divided into three layers from mould side to steel shell side: fine crystalline layer, dendrite crystalline layer and glassy layer for sample B or glassy/crystalline mixing layer for sample A.

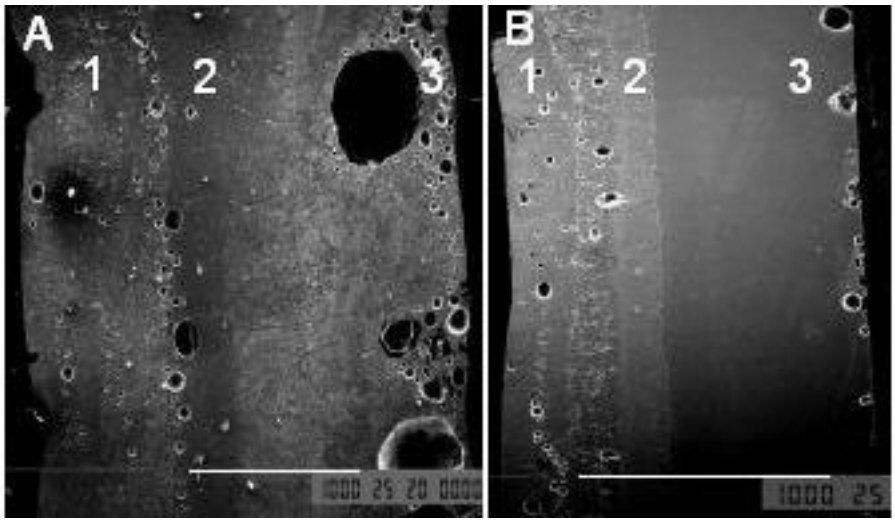

Fig.2 Cross-sectional microstructures of samples A and B. Left: mould side, right: shell side. 1: fine crystalline layer, 2: dendrite crystalline layer, 3: glassy layer for sample B or glassy/crystalline mixing layer for sample A

There are many pores in the fine crystalline layer (near mould) and glassy layer (sample B) or glassy/crystalline mixing layer (sample A) (near steel shell), and almost no pores are found in the dendrite crystalline layer of both samples A and B. The more interesting phenomenon is that the dendrite layer starts from the pores in the fine crystalline layer in both samples A and B, and grows in the direction to steel shell (**Figures 2 and 3**).

The porosity characteristics are determined by image analysis as shown in **Figure 4**. The pore number in both mould side and shell side for sample A is more than that in sample B. The largest pore diameter in sample A is also much larger than that in sample B. Therefore the porosity in sample A is larger than that in sample B.

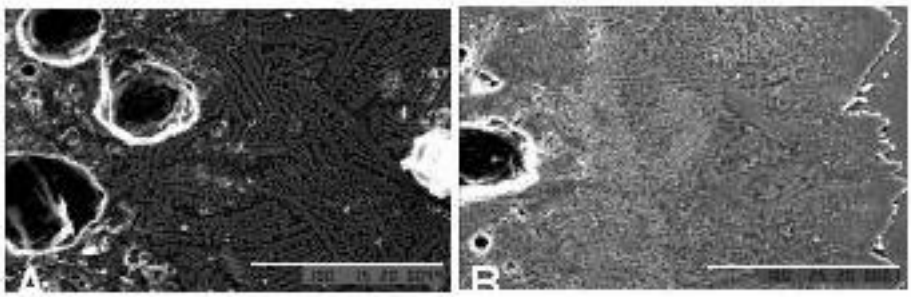

Fig.3 Photos showing the dendrite starts from the pores in both samples A and B.

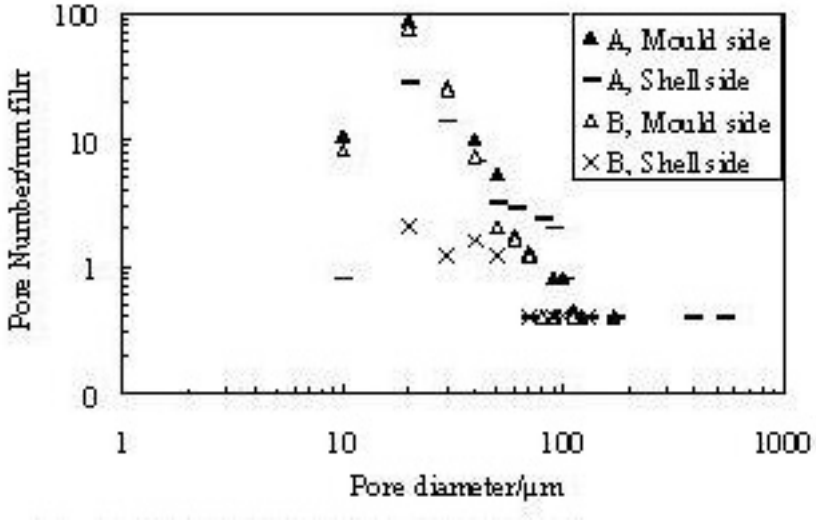

Fig 4 Porosity in mould fluxes films A and B

3.3 Crystallinity

The crystallinity of mould flux films for different steel grades was determined by direct observation (Optical microscopy and SEM) and comparative method (DPSC). The crystallinity of sample A for casting MC steel is 90% determined in this work, much higher than that of sample B, 30% for casting LC steel.

The two sides of both mould flux films A and B were investigated using XRD analysis, and mineralogical phases are shown in **Figure 5**. For sample A, mineralogical phases in both sides are cuspidine ($3CaO\ 2SiO_2\ CaF_2$) and fluorite (CaF_2), while for sample B, the side against mould is composed of cuspidine and fluorite, and the side against steel shell is glassy with little cuspidine.

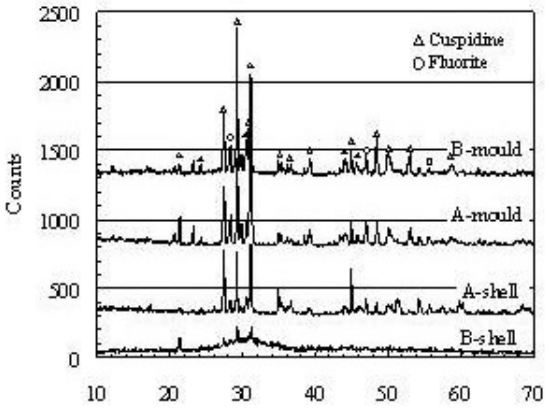

Fig 5 – X-Ray Diffraction for mould flux films A and B

3.4 Thickness of liquid layer against steel shell

The thickness of liquid layer against the steel shell is interesting because the lubrication of the steel shell is accomplished through this liquid layer. The thickness of the liquid layer can be determined from the mould flux film taken from industrial continuous casters.(Nakajima, Hiraki et al. 1994; Bezerra, Afrange et al. 2002)
In this work, the liquid layer is defined to be the layer from the front of dendrite to the strand surface in the microstructural photos.

For the mould flux film with low crystallinity (sample B), the layer from the front of dendrite to the strand surface is completely glass after cooled. The thickness of this glassy layer in the sample after cooled can be considered to be the thickness of liquid layer as shown in **Figure 2**. The thickness of liquid layer is about 0.6-0.9 mm for mould flux film B.

For the mould flux with high crystallinity (sample A), there is no complete glassy layer against the strand. The layer from the front of dendrite to the strand surface is a mixing layer of glass and crystalline. The thickness of this layer is determined to be 0.1-0.4 mm for mould flux film A.

3.5 Element Distribution

Element mapping was conducted for the whole cross section of both samples A and B (**Figure 6**). The mapped elements were oxygen (O), fluorine (F), sodium (Na), magnesium (Mg), aluminium (Al), Silicon (Si) and calcium (Ca).

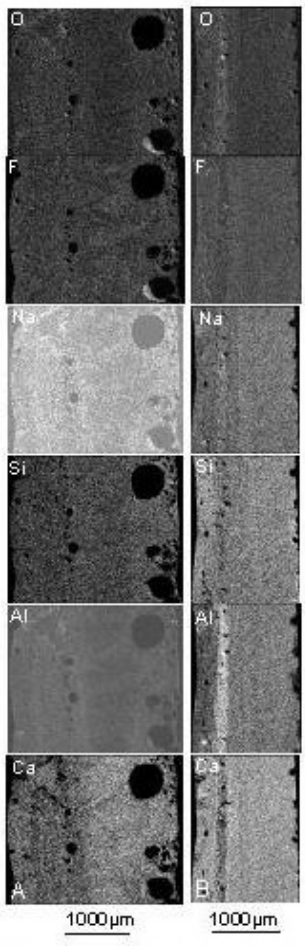

Fig 6 – Element Mapping for the whole cross

It has been shown that there is no difference for the compositions of elements O, F, Na, Si, Al and Ca in the whole cross section of sample A. But for sample B for casting LC steel, there is a thin layer with high Al, Na and lower Ca and F (**Fig.7**). This layer is just in the conjunction of fine crystalline layer and dendrite crystalline layer. Therefore, combined with the SEM image, the sample B can be considered to consist of four layers from mould side to steel shell side: fine crystalline layer, Al rich layer, dendrite layer and glassy layer.

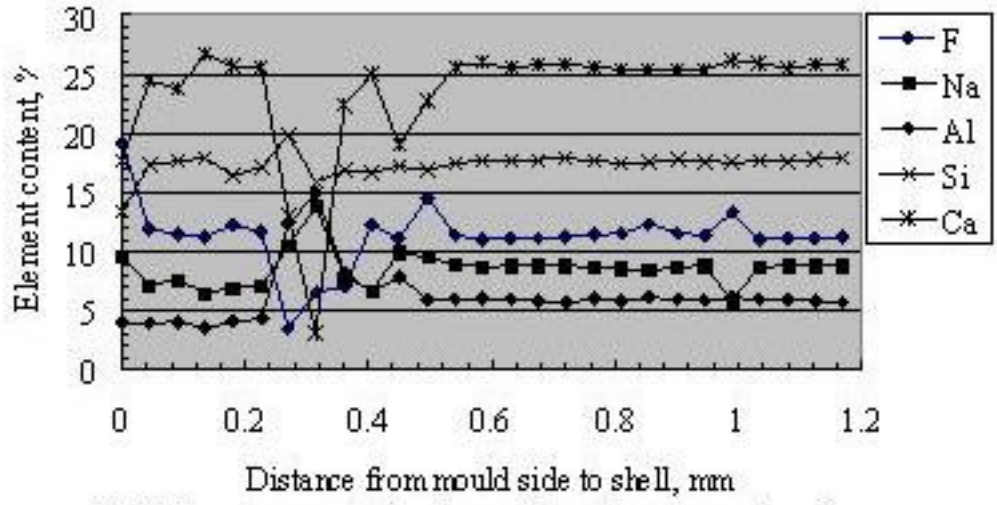

Fig 7 – Element Concentration change along the cross section of mould flux film B

The chemical composition in both phases of crystalline and glassy matrix was also analysed for sample A as shown in **Table 2** and **Fig.8**. It has been found that calcium (Ca) is always concentrated in the crystalline regions and sodium (Na) and aluminium (Al) in the glassy phases. The mole ratio of Ca:F:Si for dendrite is 0.96:0.58:0.51=1.88:1.14:1.0, which is very near the mole ratio of these elements in the cuspidine ($3CaO\cdot 2SiO_2\cdot CaF_2$), It proves that the crystalline is cuspidine.

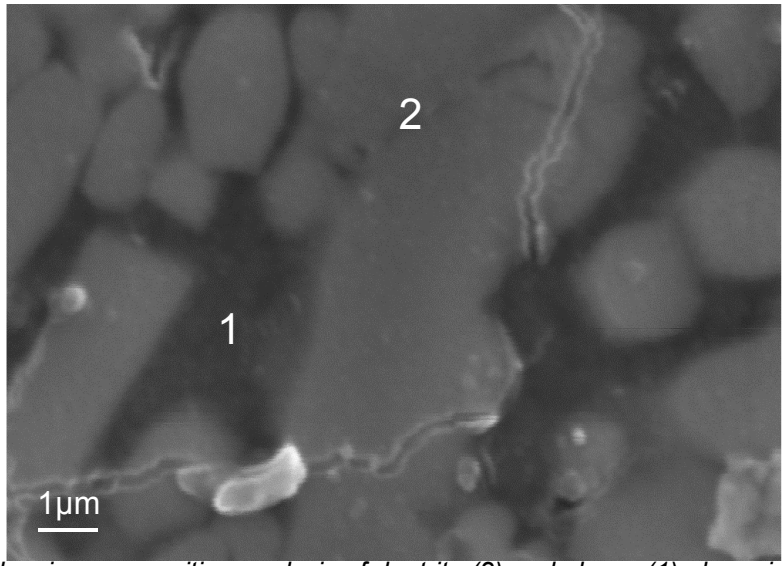

Fig. 8 – SEM photo showing composition analysis of dentrite (2) and glassy (1) phase in sample A

Table 2 - Chemical compositions of dendrite and glassy phase in sample A.

		O	F	Na	Si	Al	Ca
Dendrite (zone 2)	Range,% Average,% Mole No.	20.36-25.86 (20.24) *(1.27)*	18.85-24.54 (22.38) *(0.58)*	0.52-0.85 (0.56)	13.39-15.73 (14.17) *(0.51)*	0.89-1.77 (1.44)	36.37-40.58 (38.38) *(0.96)*
Glassy (zone 1)	Range,% Average,%	12.74-13.82 (13.36)	27.55-32.45 (30.26)	1.44-3.28 (2.28)	13.25-16.73 (14.80)	6.64-11.31 (8.34)	23.19-31.31 (28.84)

5. DISCUSSION

The surface against mould of sample A for casting MC steel is rougher with wave than that of sample B for casting LC steel. Watanabe *et al.*(Watanabe., Makoto et al. 1997) observed the change of the surface texture of the powder plate by crystallisation with a laser microscope. They found that the surface started to wave when the glass changed to crystal above 830K. It is supposed that the wave on the surface of powder film caused an increase in the interfacial thermal resistance.

The network cracks in the surface against mould for sample A may be caused by the shrinkage due to larger volumetric ratio and faster growth rate of primary cuspidine for MC steel than for LC steel. The thermal expansion due to the different expansion coefficients between crystalline and glass may be also one of the reasons(Courtney, Nuortie-Perkkio et al. 2001). Cho and Shibata(Cho and Shibata 2001) observed the shrinkage due to the crystallisation is more for mould flux for casting MC steel than that for casting LC steel using a confocal scanning laser microscope with an infrared furnace. This difference implies that the thermal resistance at mould/flux film interface arises from the solidification and crystallisation of the flux film.

The crystallinity of mould flux film A, 90% is much higher than that of mould flux film B, 30%. Crystalline phase may act as a barrier that effectively shields the radiative heat transfer. Therefore, mould flux with high crystallinity is designed for casting medium carbon steel, while low crystallinity mould flux for casting low carbon steel.

The horizontal heat transfer between the steel shell and the mould has a critical effect on process control. The overall thermal resistance (R_{tot}) between the mould and shell is given by:

$$R_{tot} = R_{Cu/sl} + (d/k)_{gl} + (d/k)_{crys} + (d/k)_{l} \quad (1)$$

where *R* is the thermal resistance, *k* the thermal conductivity, *d* the thickness of layer and the subscripts, *l*, *crys*, *gl* and *sl* refer to liquid , crystalline, glassy and slag respectively, and *Cu* to the copper mould.

The two largest terms affecting the horizontal heat flux between steel shell and mould are (i) the interfacial resistance $R_{cu/sl}$ at the slag film/mould interface, and (ii) the resistance of the solid layer $\{(d/k)_{gl} + (d/k)_{crys}\}$. Furthermore, it has been shown that $R_{Cu/sl}$ increases as (i) the thickness of solid layer increases and (ii) the amount of crystalline phase in the slag film increases.(Cho, Shibata et al. 1998)

Compared to mould flux film for casting LC steel, the mould flux film for casting MC steel has rougher surface, network cracks in the surface against mould, thicker solid layer, and much higher crystallinity, which result in higher thermal resistance to meet the requirements for casting MC steel.

All these differences arisen from the solidification and crystallisation of the flux films can be attributed to the differences in chemical compositions. Li *et al.*(Li, Thackray et al. 2004) use modified *NBO/T* as an index to express the effect of

chemical compositions on the crystallisation behaviour of mould fluxes. *NBO/T*, *i.e.* the number of non-bridging oxygen per tetrahedrally-coordinated atom, has been adopted to present the degree of depolymerisation of silicate slags (Mills 1993), and has been modified by Li *et al.*(Li, Thackray et al. 2004) as follows:

$$NBO/T = \frac{2x_{CaO} + 2x_{BaO} + 2x_{CaF_2} + 2x_{Na_2O} - 2x_{Al_2O_3} + 6x_{Fe_2O_3} + (2x_{MgO} + 2x_{MnO})}{x_{SiO_2} + 2x_{Al_2O_3} + x_{TiO_2} + 2x_{B_2O_3} + (x_{MgO} + x_{MnO})} \quad (2)$$

where x_i is the mole fraction of the component *i* in the mould flux. The bracket in the denominator/numerator means it will be included into the denominator if MgO is larger than 7.0% and or MnO is larger than 4.0%, otherwise it will be included in the numerator.

There is a good relationship between the % crystallinity and the modified *NBO/T* (***eq.(3)***). The critical point occurs at *NBO/T*=2.0. Below this critical point, the slag samples are completely glassy (very low % crystallinity), whilst above this point, the % crystallinity increases linearly with increasing the modified modified *NBO/T*.

$$\%\ crystallinity = 141.1(NBO/T) - 284.0 \quad (3)$$

According to the equations (2) and (3), The *NBO/T* value for mould fluxes A and B is 2.66 and 2.34 respectively. The %crystallinity for mould fluxes A and B calculated by equation (3) is 91% and 46% respectively which is consistent with that determined in this work.

Therefore, the characteristic differences of mould flux films for casting MC and LC steels such as surface roughness, network cracks, crystallinity and solid thickness *etc.* arise from the solidification and crystallisation of mould fluxes, and are attributed to the chemical compositions of mould fluxes.

From the observation of mould flux films A and B, the behaviour of mould flux film relating to crystallisation and porosity may be considered as follows (**Fig.9**):

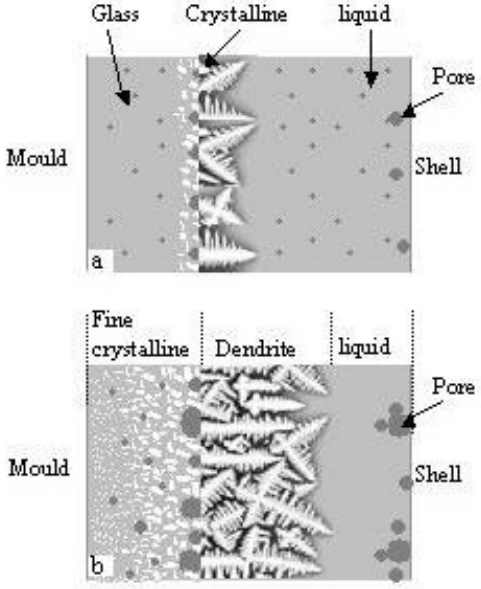

Fig 9 – Schematic Diagram showing the mechanism of crystallization and porosity formation
a: Just after the infiltration of mould flux
b: After a long time annealing of mould flux film

After the molten mould flux infiltrates into the gap between the water-cooled copper mould and the steel shell, the mould flux film was formed with a glass layer near mould side and a liquid layer near the steel shell, and gas bubbles disperse in the whole flux film (**Fig. 9(a)**). In the mould flux film from the mould to shell, there is a point that the condition (temperature *etc.*) is suitable for crystalline nucleation and

growth. This point should correspond to the nose point in the TTT curve(Kashiwaya, Cisutti et al. 1998). From this point the cuspidine nucleates and grows to dendrite crystalline in the direction to shell side. From this point to mould side, the fast-cooled glassy layer crystallises due to a long time annealing at the temperature of above 600 C and the crystalline size decreases in the direction to mould (**Fig.9(b)**).

The gas bubbles entrapped in the fast-cooled layer (then fine crystalline layer) can not escaped from this layer due to fast cooling and also due to the obstruction of the formed dendrite crystalline.

In the liquid layer against steel shell, the gas bubbles coalesce and move in the direction to steel shell as the dendrite grows. So the pore (average size) against steel shell side is larger than that in the fine crystalline layer. Finally the pores are formed by the fast cooling of the mould flux film due to the separation of steel shell from mould flux films.

The porosity of mould flux films is also related to the chemical composition of mould fluxes. Compared to mould flux B, mould flux A has higher break temperature which promotes its crystallisation. The higher crystallinity and viscosity (1300 C) also promote the entrapment of gas bubbles in the flux film.

It is anticipated to know whether the pores are formed by the crystallisation process or the pores promote the formation of crystalline. The phenomenon that there are no pores in the dendrite layer seems to prove that the pores should not be formed by crystallisation. On the other hand, the pores may promote the crystallisation as nuclei site of heterogeneous nucleation as the dendrite starts from the pores in the fine crystalline layer.

The pores (gas bubbles) may come from carbon oxidation, fluorine evaporation in the mould flux, or the reactions between mould flux and molten steel, or injected Argon gas bubbles. But it is not easy to determine the source of gas bubbles only through the investigation on mould flux films.

In this work, combined SEM observation and SEM-EDS analysis, sample A for casting MC steel was found to consist of three layers from mould side to steel shell: fine crystalline layer, dendrite layer and glassy-crystalline layer for sample A. It is consistent with that by Tarrant and Brooks(Tarrant and Brooks 2003).

Microanalysis and XRD analysis show that the crystalline is cuspidine which is consistent with the other results(Grieveson, Bagha et al. 1988; Bezerra, Afrange et al. 2002; Tarrant and Brooks 2003) that cuspidine is always present for fluorine-containing mould flux. But CaF_2 is also found in this work.

For sample B, it consists of four layers: fine crystalline layer, Al-rich layer, dendrite layer and glassy layer. Hooli(Hooli 2002) found five layers in the slag film of 390 mm below meniscus: Na, F rich layer (50%Na), Al rich layer, Ca rich layer, thin layer with coarse structure and liquid layer (layer solidified during tailout). But in this study, from element mapping through the whole cross section of both samples A and B, the Na, F rich layer and Ca rich layer were not detected.

Nakajima *et al.* **(Nakajima, Hiraki et al. 1994)** determined the relationship between the casting speed and the thickness of liquid layer in the mould flux film. According to the relationship by Nakajima *et al.* **(Nakajima, Hiraki et al. 1994), t**he thickness of liquid layer is estimated to be 0.4 mm and 0.3 mm for mould flux films A and B respectively. It is different from that determined in this work.

It should be noticed that Nakajima *et al.* **(Nakajima, Hiraki et al. 1994)** took the mould flux films just below the mould by a film-sampling apparatus while the mould flux films were taken at around 300 mm from the top of the mould. The crystallisation changes along the position of mould flux film in the mould. The crystallinity increases

from meniscus to the bottom of mould: liquid slag--100% glassy, near meniscus--40%glass, and 30cm below meniscus--30%glassy (Courtney, Nuortie-Perkkio et al. 2001). Therefore, the thickness of liquid layer decreases as the mould flux film moves away from the meniscus to the end of the mould due to the increase in the thickness of dendrite crystalline layer.

6. CONCLUSIONS

The following conclusions can be obtained from this study:

(1) The mould flux film for casting MC steel consists of three layers from mould side to steel shell side: fine crystalline layer, dendrite layer and glassy/crystalline mixing layer. But the flux film for casting LC steel is composed of four layers: fine crystalline layer, thin Al-rich layer, dendrite layer and glassy layer.
(2) XRD and EDS analysis show that the crystalline phase is mainly composed of cuspidine ($3CaO\cdot 2SiO_2\cdot CaF_2$).
(3) Mould flux film for casting MC steel is up to 1.5 times thicker than that for casting LC steel.
(4) Pores in the diameter from 5μm to 550μm were found in the fine crystalline layer and glassy layer in both samples fro casting MC and LC steels, but not detected in the dendrite crystalline layer.
(5) There are network cracks, 0.47 mm/mm^2, in the depth of less than 1.0 mm in the mould flux film for casting MC steel, but it is not found in the surface of the film for casting LC steel.
(6) The %crystalinity in the mould flux film for casting MC steel is 90%, much higher than that of mould flux film for casting LC steel, 30%.
(7) Compared to mould flux film for casting LC steel, the mould flux film for casting MC steel has the rougher surface, the network cracks in the surface against mould, the thicker crystalline layer, and the much higher crystallinity which result in higher thermal resistance to meet the requirements for casting MC steel. The characteristic differences of mould flux films for casting MC and LC steels can be attributed to the chemical compositions of the mould fluxes.
(8) The mechanism for porosity formation and crystallisation is also discussed.

7. ACKNOWLEDGEMENT

The authors would like to thank Dr. Alistair B. Fox and Richard P Thackray (Imperial College), Dr. Adrian S. Normanton and Dr Shahid Riaz (Corus UK) for their kind suggestions. They also acknowledge funding from EPSRC.

8. References

Bezerra, M. C. C., O. D. C. Afrange, et al. (2002). Evaluation of solidified slag films fof mould fluxes used in continuous casting of steel, taken from slab mould interface. Mills Symposium, The Institute of Materials, London, UK.

Cho, J. W. and H. Shibata (2001). "Effect of solidification of mold fluxes on the heat transfer in casting mold." Journal of Non-Crystalline Solids **282**(1): 110-117.

Cho, J. W., H. Shibata, et al. (1998). "Thermal resistance at the interface between mould flux film and mould for continuous casting of steels." ISIJ International **38**(5): 440-446.

Courtney, L., S. Nuortie-Perkkio, et al. (2001). "Crystallisation of slag films formed in continuous casting." Ironmaking and Steelmaking **28**(5): 412-417.
Grieveson, P., S. Bagha, et al. (1988). "Physical properties of casting powders: part 2 Mineralogical constitution of slags formed by powders." Ironmaking and Steelmaking **15**(4): 181-186.
Hooli, P. O. (2002). "Mould flux film between mould and steel shell." Ironmaking and Steelmaking **29**(4): 293-296.
Kashiwaya, Y., C. E. Cisutti, et al. (1998). "An investigation of the crystallisation of a continuous casting mould slag using the single hot thermocouple technique." ISIJ International **38**(4): 357-365.
Li, Z., R. Thackray, et al. (2004). A test to determine the crystallinity of mould fluxes. VII International Conference on Molten Slags Fluxes and Salts, Cape Town, South Africa.
Mills, K. (1993). "The influence of structure on the physico-chemical properties of slags." ISIJ International **33**(1): 148-155.
Nakajima, K., S. Hiraki, et al. (1994). "Influence of Mold heat flux on longitudinal surface cracks during high-speed continuous casting of steel slab." The Sumitomo Search(55): 32-39.
Susa, M., K. C. Mills, et al. (1994). "Thermal properties of slag films taken from continous casting mould." Iron and steelmaker **21**(4): 279-286.
Tarrant, B. and G. Brooks (2003). "Solidification of industrial mould fluxes." Iron and steelmaker **30**(5): 52-60.
Watanabe., K., S. Makoto, et al. (1997). "The effect of crystallization of mold powder on the heat transfer in continuous casting mold." Tetsu-to-Hagane **83**(2): 115-120.